Energetics and Mechanism of Organolanthanide-Mediated Phosphinoalkene Hydrophosphination/Cyclization. A Density Functional Theory Analysis

Alessandro Motta, Ignazio L. Fragalà,*,† and Tobin J. Marks*,‡

Dipartimento di Scienze Chimiche, Università di Catania, and INSTM, UdR Catania, Viale A. Doria 6, 95125 Catania, Italy, and Department of Chemistry, Northwestern University, Evanston, Illinois 60208-3113

Received July 8, 2005

This contribution focuses on organolanthanide-mediated hydrophosphination processes and analyzes the hydrophosphination/cyclization of a prototypical phosphinoalkene, $H_2P(CH_2)_3$-$CH{=}CH_2$, catalyzed by $Cp_2LaCH(TMS)_2$, using density functional theory methods, and compares/contrasts the results to analogous hydroamination/cyclization processes. The reaction is found to proceed in two discrete steps: namely, cyclization via C=C insertion into the Cp_2La-P(phosphido) linkage to form La−C and C−P bonds and subsequent La−C protonolysis. Calculations have been carried out for: (i) insertion of the olefinic moiety into the La−P bond and (ii) La−C protonolysis by a second substrate molecule. The cyclized phosphinoalkane is released in the latter process and the active catalyst regenerated. DFT energetic profiles have been generated for the entire catalytic cycle. DFT-derived geometries and stabilities of reactants, intermediates, and products have also been analyzed. The picture that emerges is one of approximately thermoneutral insertion of the alkene fragment into the Cp_2La-P(phosphido) bond via a highly organized, seven-membered chairlike cyclic transition state. The resulting cyclopentylmethyl complex then undergoes turnover-limiting but exothermic protonolysis to yield a phosphine−phosphido complex, the likely resting state of the catalyst. Interestingly, this energetic ordering of barriers is *exactly reversed* from that in the formally analogous hydroamination/cyclization process, where C=C insertion is turnover-limiting and protonolysis rapid. The calculations provide evidence that, in the hydrophosphination/cyclization process, there is competition at the lanthanide center between cyclized product and incoming unconverted substrate and, therefore, some inhibition of the protonolysis step, in accord with experiment. Parallel calculations demonstrate that such effects are not generally important in the analogous hydroamination/cyclization process. Derived thermodynamic and kinetic parameters are in excellent agreement with experiment.

Introduction

The implementation of organolanthanide catalysts to effect a wide variety of synthetically useful catalytic transformations is rapidly growing in scope and diversity.[1] Organolanthanides have been successfully applied to the chemo-, regio-, and enantioselective catalytic hydrogenation of olefins, alkynes, and imines,[2] hydrosilylation of olefins and alkynes,[3] hydroboration of olefins,[4] various types of polymerizations and copolymerizations,[2d,5] and, in particular, to the hydroamination/cyclization/bicyclization of aminoalkenes,[6,7] aminoalkynes,[8] aminoallenes,[9] and aminodienes,[10] as well as

* To whom correspondence should be addressed. E-mail: lfragala@dipchi.unict.it (I.L.F.); t-marks@northwestern.edu (T.J.M.).
† Università di Catania.
‡ Northwestern University.

(1) For recent organolanthanide reviews, see: (a) Hong, S.; Marks, T. J. *Acc. Chem. Res.* **2004**, *37*, 673−686. (b) Aspinall, H. C. *Chem. Rev*. **2002**, *102*, 1807−1850. (c) Edelmann, F. T.; Freckmann, D. M. M.; Schumann, H, *Chem. Rev.* **2002**, *102*, 1851−1896. (d) Arndt, S.; Okuda, J. *Chem. Rev.* **2002**, *102*, 1953−1976. (e) Molander, G. A.; Romero, A. C. *Chem. Rev.* **2002**, *102*, 2161−2186. (f) Shibasaki, M.; Yoshikawa, N. *Chem. Rev.* **2002**, *102*, 2187−2210. (g) Inanaga, J.; Furuno, H.; Hayano, T. *Chem. Rev.* **2002**, *102*, 2211−2226. (h) Molander, G. A. *Chemtracts: Org. Chem.* **1998**, *18*, 237−263. (i) Edelmann, F. T. *Top. Curr. Chem.* **1996**, *179*, 247−276. (j) Edelmann, F. T. In *Comprehensive Organometallic Chemistry*; Wilkinson, G., Stone, F. G. A., Abel, E. W., Eds.; Pergamon Press: Oxford, U.K., 1995; Vol. 4, Chapter 2. (k) Schumann, H.; Meese-Marktscheffel, J. A.; Esser, L. *Chem. Rev.* **1995**, *95*, 865−986. (l) Schaverien, C. J. *Adv. Organomet. Chem.* **1994**, *36*, 283−362. (m) Evans, W. J. *Adv. Organomet. Chem.* **1985**, *24*, 131−177. (n) Marks, T. J.; Ernst, R. D. In *Comprehensive Organometallic Chemistry*; Wilkinson, G., Stone, F. G. A., Abel, E. W., Eds.; Pergamon Press: Oxford, U.K., 1982; Chapter 21.

(2) Hydrogenation: (a) Obora, Y.; Ohta, T.; Stern, C. L.; Marks, T. J. *J. Am. Chem. Soc*. **1997**, *119*, 3745−3755. (b) Roesky, P. W.; Denninger, U.; Stern, C. L.; Marks, T. J. *Organometallics* **1997**, *16*, 4486-4492. (c) Haar, C. M.; Sern, C. L.; Marks, T. J. *Organometallics* **1996**, *15*, 1765−1784. (d) Jeske, G.; Lauke, H.; Mauermann, H.; Swepston, P. N.; Schumann, H.; Marks, T. J. *J. Am. Chem. Soc.* **1985**, *107*, 8091−8103.

(3) Hydrosilylation: (a) Horino, Y.; Livinghouse, T. *Organometallics* **2004**, *23*, 12−14. (b) Molander, G. A.; Corrette, C. P. *Organometallics* **1998**, *17*, 5504−5512. (c) Schumann, H.; Keitsch, M. R.; Winterfeld, J.; Muhle, S.; Molander, G. A. *J. Organomet. Chem.* **1998**, *559*, 181−190. (d) Fu, P.-F.; Brard, L.; Li, Y.; Marks, T. J. *J. Am. Chem. Soc.* **1995**, *117*, 7157−7168. (e) Molander, G. A.; Julius, M. *J. Org. Chem.* **1992**, *57*, 6347−6351. (f) Sakakura, T.; Lautenschlager, H.; Tanaka, M. *J. Chem. Soc., Chem. Commun.* **1991**, 40−41.

(4) Hydroboration: (a) Molander, G. A.; Pfeiffer, D. *Org. Lett*. **2001**, *3*, 361−363. (b) Bijpost, E. A.; Duchateau, R.; Teuben, J. H. *J. Mol. Catal.* **1995**, *95*, 121−128. (c) Harrison, K. N.; Marks, T. J. *J. Am. Chem. Soc.* **1992**, *114*, 9220−9221.

10.1021/om050570d CCC: $30.25
Publication on Web 09/13/2005

recently to the hydrophosphination/cyclization of alkenes and alkynes.[11] Of these transformations, olefin hydrophosphination has proven particularly difficult to accomplish with typical late-transition-metal catalysts.[12] However, the stereoelectronic tunability of organolanthanide coordination spheres, coupled with high electrophilicity, absence of conventional oxidative addition/reductive elimination pathways, and high kinetic lability, suggest an attractive alternative pathway for accomplishing this transformation. Moreover, cyclic phosphines are as yet relatively understudied[13] and may have applications as ligands similar to all-carbon ligands[14] or display interesting pharmacological properties.[15] In addition, phosphorus heterocycles produced in hydrophosphination/cyclization processes offer attractive building blocks for classes of electron-rich chiral ligands that have been utilized extensively for asymmetric transformations.[16]

Scheme 1. Proposed Catalytic Cycle for the Organolanthanide-Catalyzed Cyclohydrophosphination of Phosphinoalkenes

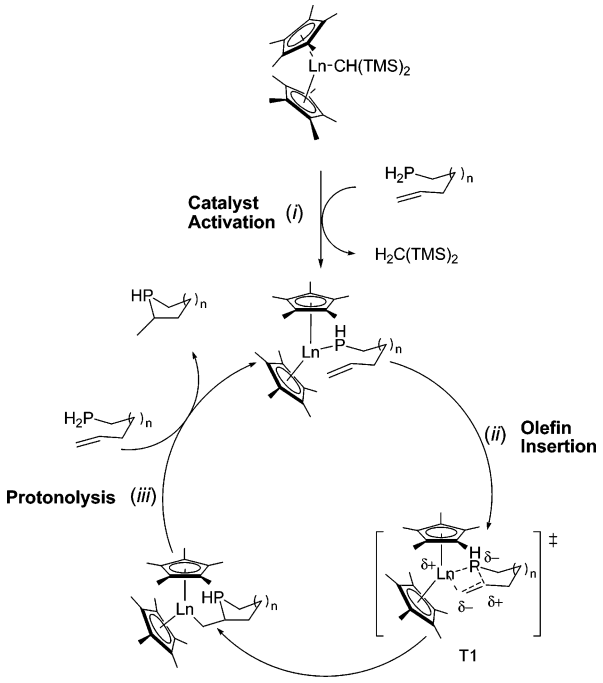

Olefin hydrophosphination, which in a formal sense consists of the addition of a P−H bond across a C=C bond, analogously to hydroamination, is a transformation of seemingly fundamental simplicity and atom economy (eq 1) and would appear to offer an attractive route to numerous classes of organophosphorus molecules. An approximate thermodynamic analysis[17] based

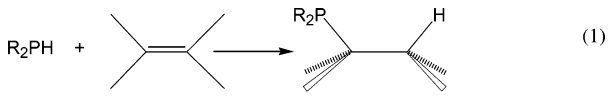

(1)

on tabulated bond enthalpies for simple phosphines indicates that a catalytic cycle similar to that of hydroamination[1a] may also be possible for the hydrophosphination case. In such a scenario, after initial protonolysis of the precatalyst (Scheme 1, step i), insertion of carbon−carbon unsaturation into the resulting lanthanide−phosphido bond (Scheme 1, step ii) should be approximately thermoneutral for an alkene ($\Delta H \approx +2$ kcal/mol) and can be coupled with subsequent exothermic ($\Delta H \approx -17$ kcal/mol) Ln−C protonolysis to constitute an efficient catalytic P−C bond-forming cycle (Scheme 1, step iii). While certainly appealing, many aspects of this hypothetical hydroamination-like pathway raise questions which can be best addressed by theory, including the role of the very different relative chemistries and energetics of N−H/P−H, N−C/P−C,

(5) (a) Koo, K.; Fu, P.-F.; Marks, T. J. *Macromolecules* **1999**, *32*, 981−988. (b) Jia, L.; Yang, X.; Seyam, A. M.; Albert, I. D. L.; Fu, P.-F.; Yang, S.; Marks, T. J. *J. Am. Chem. Soc*. **1996**, *118*, 7900−7913. (c) Jeske, G.; Schock, L. E.; Mauermann, H.; Swepston, P. N.; Schumann, H.; Marks, T. J. *J. Am. Chem. Soc.* **1985**, *107*, 8103−8110. (d) Watson, P. L. *J. Am. Chem. Soc.* **1982**, *104*, 337−339.

(6) (a) Ryu, J.-S.; Marks, T. J.; McDonald, F. E. *J. Org. Chem.* **2004**, *69*, 1038−1052. (b) Gribkov, D. V.; Hampel, F.; Hultzsch, K. C. *Eur. J. Inorg. Chem.* **2004**, 4091−4101. (c) Kim, Y. K.; Livinghouse, T.; Horino, Y. *J. Am. Chem. Soc.* **2003**, *125*, 9560−9561. (d) Ryu, J.-S.; McDonald, F. E.; Marks, T. J. *Org. Lett.* **2001**, *3*, 3091−3094. (e) Kim, Y. K.; Livinghouse, T.; Bercaw, J. E. *Tetrahedron Lett.* **2001**, *42*, 2933−2935. (f) Molander, G. A.; Dowdy, E. D. *J. Org. Chem.* **1999**, *64*, 6515−6517. (g) Molander, G. A.; Dowdy, E. D. *J. Org. Chem.* **1998**, *63*, 8983−8988.

(7) (a) Gagné, M. R.; Stern, C. L.; Marks, T. J. *J. Am. Chem. Soc.* **1992**, *114*, 275−294. (b) Gagné, M. R.; Marks, T. J. *J. Am. Chem. Soc.* **1989**, *111*, 4108−4109. (c) Giardello, M. A.; Conticello, V. P.; Brard, L.; Gagné, M. R.; Marks, T. J. *J. Am. Chem. Soc.* **1994**, *116*, 10241−10254. (d) O'Shaughnessy, P. N.; Knight, P. D.; Morton, C.; Gillespie, K. M.; Scott, P. *Chem. Commun.* **2003**, 1770−1771. (e) Kim, J. Y.; Livinghouse, T. *Org. Lett.* **2005**, *7*, 1737−1739.

(8) (a) Li, Y.; Marks, T. J. *J. Am. Chem. Soc.* **1998**, *120*, 1757−1771. (b) Li, Y.; Marks, T. J. *J. Am. Chem. Soc.* **1996**, *118*, 9295−9306. (c) Li, Y.; Marks, T. J. *Organometallics* **1996**, *15*, 3370−3372. (d) Li, Y.; Marks, T. J. *J. Am. Chem. Soc.* **1996**, *118*, 707−708. (e) Li, Y.; Fu, P.-F.; Marks, T. J. *Organometallics* **1994**, *13*, 439−440.

(9) (a) Arredondo, V. M.; McDonald, F. E.; Marks, T. J. *Organometallics* **1999**, *10*, 1949−1960. (b) Arredondo, V. M.; Tian, S.; McDonald, F. E.; Marks, T. J. *J. Am. Chem. Soc.* **1999**, *121*, 3633−3639. (c) Arredondo, V. M.; McDonald, F. E.; Marks, T. J. *J. Am. Chem. Soc.* **1998**, *120*, 4871−4872.

(10) (a) Hong, S.; Kawaoka, A. M.; Marks, T. J. *J. Am. Chem. Soc.* **2003**, *125*, 15878−15892. (b) Hong, S.; Marks, T. J. *J. Am. Chem. Soc.* **2003**, *124*, 7886−7887.

(11) Hydrophosphination: (a) Kawaoka, A.; Marks, T. J. *J. Am. Chem. Soc.* **2005**, *127*, 6311−6324. (b) Kawaoka, A. M.; Marks, T. J. *J. Am. Chem. Soc.* **2004**, *126*, 12764−12765. (c) Kawaoka, A. M.; Douglass, M. R.; Marks, T. J. *Organometallics* **2003**, *22*, 4030−4032. (d) Douglass, M. R.; Stern, C. L.; Marks, T. J. *J. Am. Chem. Soc.* **2001**, *123*, 10221−10238. (e) Douglass, M. R.; Marks, T. J. *J. Am. Chem. Soc.* **2000**, *122*, 1824−1825.

(12) Hydrophosphination mediated by Pd, Pt, and Ni complexes: (a) Kovacik, I.; Wicht, D. K.; Grewal, N. S.; Glueck, D. S.; Incarnito, C. D.; Guzei, I. A.; Rheingold, A. L. *Organometallics* **2000**, *19*, 950−953. (b) Wicht, D. K.; Kourkine, Kovacik, I.; Glueck, D. S.; Cancolina, T. E.; Yap, G. P. A.; Incarnito, C. D.; Rheingold, A. L. *Organometallics* **1999**, *18*, 5381−5394. (c) Costa, E.; Pringle, P. G.; Worboys, K. *Chem. Comm*. **1998**, 49−50. (d) Wicht, D. K.; Kourkine, I. V.; Lew, B. M.; Nthenge, J. M.; Glueck, D. S. *J. Am. Chem. Soc.* **1997**, *119*, 5039−5040. (e) Han, L.-B.; Tanaka, M. *J. Am. Chem. Soc.* **1996**, *118*, 1571−1572. (f) Using no transition-metal catalyst: Gaumont, A.-C.; Simon, A.; Denis, J.-M. *Tetrahedron Lett*. **1998**, *39*, 985−988.

(13) (a) Quin, L. D.; Hughes, A. N. In *The Chemistry of Organophosphorous Compounds*; Hartley, F. R., Ed.; Wiley: Chichester, U.K., 1990; Vol 1, pp 295−394. (b) Quin, L. D. In *The Heterocyclic Chemistry of Phosphorus: Systems Based on the Phosphorus-Carbon Bond*; Wiley: New York, 1981.

(14) Dillon, K. B.; Mathey, F.; Nixon J. F. In *Phosphorus: The Carbon Copy*; Wiley: Chichester, U.K., 1998.

(15) Price, N. R.; Chambers, J. In *The Chemistry of Organophosphorus Compounds*; Hartley, F. R., Ed.; Wiley: Chichester, U.K., 1990; Vol 1, pp 643−661.

(16) (a) Burk, M. J. *Acc. Chem. Res*. **2000**, *33*, 363−372. (b) Burk, M. J.; Gross, M. F.; Martinez, J. P. *J. Am. Chem. Soc.* **1995**, *117*, 9375−9376. (c) Burk, M. J.; Harper, G. P.; Kalberg, C. S. *J. Am. Chem. Soc.* **1995**, *117*, 4423−4424. (d) Burk, M. J.; Feaster, J. E.; Nugent, W. A.; Harlow, R. L. *J. Am. Chem. Soc.* **1993**, *115*, 10125−10138.

(17) Data from: (a) Nolan, S. P.; Stern, D.; Hdden, D.; Marks, T. J. *ACS Symp. Ser.* **1990**, *No. 428*, 159−174. (b) Nolan, S. P.; Stern, D.; Marks, T. J. *J. Am. Chem. Soc.* **1989**, *111*, 7844−7853. (c) Skinner, H. A.; Pilcher, G. In *The Chemistry of the Metal−Carbon Bond*; Hartley, F. R., Patai, S., Eds.; Wiley: Chichester, U.K., 1982; Vol. 1, Chapter 2. (d) Goldwhite, H. *Introduction to Phosphorus Chemistry*; Cambridge University Press: Cambridge, U.K., 1981.

and Ln−N/Ln−P linkages as well as the great differences in N vs P hardness and softness. Likewise, those factors governing hydrophosphination rate, regiochemistry, and stereochemistry are poorly understood and would greatly benefit from a high-level electronic structural analysis of the reaction coordinate and transition state(s).

The fundamental understanding and exploitation of catalytic mechanisms involving lanthanide complexes has often benefited from theoretical studies.[18] The present investigation represents the first theoretical analysis of the relevant mechanistic details of phosphinoalkene hydrophosphination/cyclization mediated by Cp'_2LnR complexes ($Cp' = \eta^5$-H_5C_5; $R = CH(TMS)_2$; Ln = La). Here $(C_5H_5)_2LaCH(TMS)_2$ is adopted as the model precatalyst, while the substrate is represented by archetypical 1-phosphinopent-4-ene (CH_2=$CH(CH_2)_3$-PH_2). Experimental studies of aminoalkene hydroamination[1a,7a] reveal that the reaction proceeds equally well in pentane, toluene, benzene, and related solvents, while in donor solvents such THF, catalytic rates are significantly depressed.[7a] Since noncoordinating solvents do not significantly alter the overall reaction pathway, it will be of interest to analyze the influence of solvation on the hydrophosphination process. In the present study, the second substrate molecule involved in the protonolytic step iii following the cyclization has been modeled with the simpler methylphosphine (CH_3PH_2) molecule. There is, in fact, evidence (vide infra) that the effect of the remote CH_2=CH− unsaturation on the protonolysis pathway represents only a minor energetic factor. The geometries of the intermediates as well as of the transition states have been evaluated here to define a minimal energy reaction coordinate to compare and contrast with experimental kinetic and thermodynamic data,[11b,c] as well as to highlight the role of interactions among ligands, reactants, and product species within the lanthanide coordination sphere.

Computational Details

Calculations were performed adopting the B3LYP formalism. The effective core potential (ECP) of Hay and Wadt,[19] which explicitly treats 5s and 5p electrons and a basis set contracted as [3s, 3p, 2d, 1f], were used for the lanthanum atom. The standard all-electron 6-31G** basis was used for the remaining atoms.[20] Polarization functions are required in such calculations to obtain correct results. Molecular geometry optimization of stationary points used analytical gradient techniques. The transition state was searched with the synchronous, transit-guided quasi-Newton method.[21] IRC calculations[22] were performed to scrutinize the reaction pathway through the transition states in both the cyclization and protonolysis steps. Frequency analyses were performed in order to obtain thermochemical information about the reaction pathways at 298 K. The force constants were determined analytically. Solvent effects were modeled using the polarized continuum (overlapping spheres) formalism (PCM) of Tomasi and co-workers.[23] The PCM method models the solvent as a continuum of uniform dielectric constant, and the solute is placed into a cavity within the solvent. The cavity is constructed by placing a sphere around each solute heavy atom. Hydrogen atoms are always enclosed within the sphere of the atom to which they are bonded. For the atomic radii, the Bondi approximation was used. In this method, the effects of solvation are folded into the iterative SCF procedure. The dielectric constants of the solvents investigated are as follows: C_6H_6, 2.247; $C_6H_5CH_3$, 2.379; heptane, 1.92. All calculations were performed using G03[24] code on an IBM-SP system.

Results and Discussion

This section focuses on mechanistic and energetic aspects of the hydrophosphination/cyclization process and compares/contrasts the mechanistic pathways with those obtained in the superficially analogous hydroamination process. The resulting study affords a significantly better understanding of mechanism in this unique class of transformations, and distinctive differences between hydroamination and hydrophosphination are highlighted to understand the influence of the heteroatom (N or P) on the kinetics and thermodynamics of the catalytic cycle.

The computational data relative to the overall energetics involved in hydroamination and hydrophosphination/cyclization processes on passing from linear substrates to final cyclized products (eqs 2 and 3) reveal that the processes are exothermic for both hydroamination ($\Delta H_0 = -14.0$ kcal/mol) and hydrophosphination ($\Delta H_0 = -19.1$ kcal/mol). Thermodynamically, the hydrophosphination/cyclization is favored over hydroamination. Thus, the energetics of the process involve an interplay of E−H (E = N, P) bond-breaking, E−C bond formation, and olefin saturation. The computed energetic values are compiled in Table 1.[17]

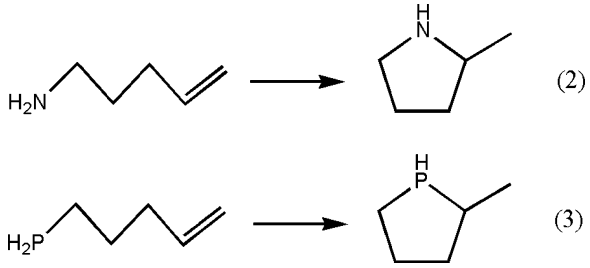

Structural distortions accompanying ring closure play an important role in the overall energetics of the product heterocycles. Formally, the N and P atoms can be described by an sp^3 hybridization model requiring 109.4° valence angles, with one sp^3 orbital occupied by a formal

(18) (a) Luo, Y.; Selvam, P.; Koyama, M.; Kubo, M.; Miyamoto, A. *Chem. Lett.* **2004**, *33*, 780−785. (b) Margl, P.; Deng, L.; Ziegler, T. *Top. Catal.* **1999**, *7*, 187−208. (c) Perrin, L.; Maron, L.; Eisenstein, O.; Schwartz, D. J.; Burns, C. J.; Andersen, R. A. *Organometallics* **2003**, *22*, 5447−5453. (d) Eisenstein, O.; Maron, L. *J. Organomet. Chem.* **2002**, *647*, 190−197. (e) Margl, P.; Deng, L.; Ziegler, T. *J. Am. Chem. Soc.* **1999**, *121*, 154−162. (f) Perrin, L.; Maron, L.; Eisenstein, O. *New J. Chem.* **2004**, *28*, 1255−1259. (g) Perrin, L.; Maron, L.; Eisenstein, O. *Inorg. Chem.* **2002**, *41*, 4355−4362. (h) Margl, P.; Deng, L.; Ziegler, T. *J. Am. Chem. Soc.* **1998**, *120*, 5517−5525.

(19) Hay, P. J.; Wadt, W. R. *J. Chem. Phys*. **1985**, *82*, 299−310.

(20) (a) Hehre, W. J.; Ditchfield, R.; Pople, J. A. *J. Chem. Phys.* **1972**, *56*, 2257−2261. (b) Francl, M. M.; Pietro, W. J.; Hehre, W. J.; Binkley, J. S.; Gordon, M. S.; DeFrees, D. J.; Pople, J. A. *J. Chem. Phys.* **1982**, *77*, 3654−3665.

(21) Peng, C.; Schlegel, H. B. *Isr. J. Chem*. **1994**, *33*, 449−454.

(22) (a) Gonzalez, C.; Schlegel, H. B. *J. Chem. Phys.* **1989**, *90*, 2154−2161. (b) Gonzalez, C.; Schlegel, H. B. *J. Phys. Chem.* **1990**, *94*, 5523−5527.

(23) (a) Miertus, S.; Tomasi, J. *Chem. Phys.* **1982,** *65*, 239−245. (b) Miertus, S.; Scrocco, E.; Tomasi, J. *Chem. Phys.* **1981,** *55*, 117−129. (c) Cossi, M.; Barone, V.; Cammi, R.; Tomasi, J. *Chem. Phys. Lett.* **1996,** *255*, 327−335. (d) Cances, M. T.; Mennucci, V.; Tomasi, J. *J. Chem. Phys.* **1997,** *107*, 3032−3041. (e) Barone, V.; Cossi, M.; Tomasi; J. *J. Comput. Chem.* **1998,** *19*, 404−417.

(24) Frisch, M. J., et al. *Gaussian 03*, Revision A.1; Gaussian, Inc., Pittsburgh, PA, 2003.

Table 1. Bond Dissociation Enthalpies at 298 K[a]

bond	enthalpy, kcal/mol
R_2N-H	100
R_2N-C	80
R_2P-H	77
R_2P-C	63

[a] Values taken from ref 17.

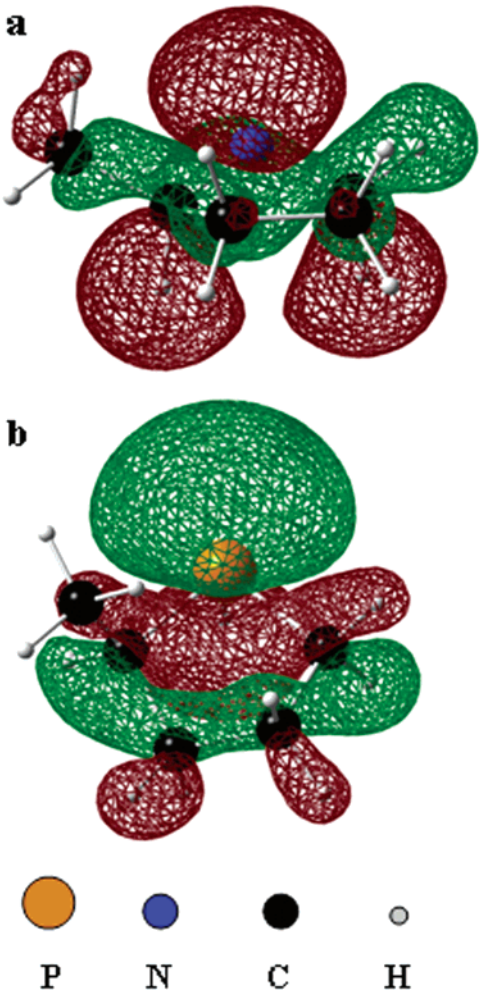

Figure 1. Isodensity HOMO surfaces in the (a, top) aminocycle and (b, bottom) phosphacycle hydroelementation products.

lone pair. In reality, isodensity plots of molecular orbitals representing the P (28a) and N (24a) lone pairs reveal that, in the case of the cyclic phosphine, the lone pair is significantly more diffuse than for the nitrogen atom[25] (Figure 1). Therefore, the valence angles around the phosphorus atom are distorted with respect to tetrahedral and exhibit an equilibrium mean value of 94.8°. Note that a similar trend is observed on passing from methylamine (valence angle 108.4°) to methylphosphine (valence angle 96.2°). It is found that the ring atoms in the aminocycle are forced to internal angles ranging between 101.9 and 105.5°, while the phosphacycle is somewhat more relaxed, principally due to the greater expansion of the phosphorus center. Thus, the presently optimized geometrical parameters for the phosphacycle indicate bond angles nearer to classical values, including simple phosphines. The internal angles around the carbon atoms range from 105.1 to 108.1°, while the internal C−P−C angle is 92.5°. For these reasons, differences in the energetics of the bond-forming/bond-breaking process and of the ring closure energetics account for the greater exothermicity of the hydrophosphination/cyclization process relative to hydroamination/cyclization.

The products of the present study exist in two diastereomeric conformers, cis and trans, relating to the relative orientations of the C−methyl and the E−H bond vectors. In the aminocycle, the two conformers are

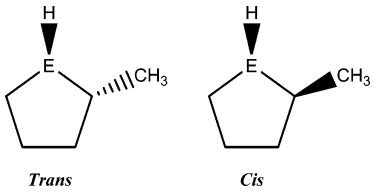

similar in energy (ΔE = 0.1 kcal/mol) and doubtless undergo rapid interconversion via inversion at nitrogen, while in the phosphacycle, the cis conformer is slightly more stable than the trans conformer (ΔE = 1.1 kcal/mol), and inversion at phosphorus is relatively slow.[11b,c]

Precatalyst Activation Process. The mechanistic and kinetic aspects of precatalyst activation will be discussed in conjunction with Ln−C protonolysis (vide infra). In this section, the focus is on proton transfer between substrate and precatalyst (eqs 4 and 5). This

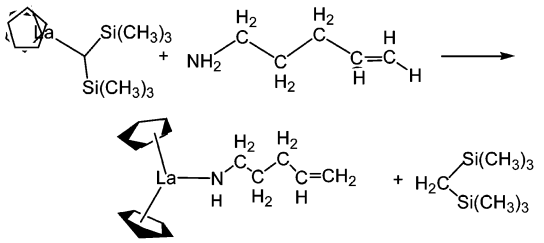

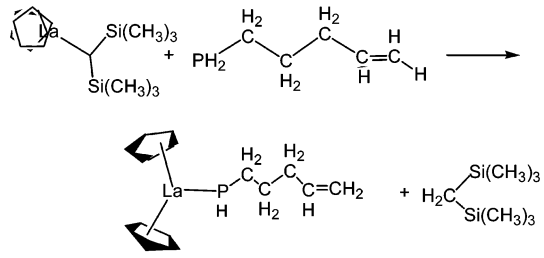

reaction affords $CH_2(TMS)_2$ and a lanthanocene phosphido complex, which represents the starting point of the catalytic cycle. Experimentally, there is evidence that the rapid, quantitative activation in the hydroamination case[7a] does not find a counterpart in the analogous hydrophosphination,[11b,c] which is significantly more sluggish and usually requires alternative activation procedures to initiate the catalytic cycle: e.g., using a hydride produced in situ from a lanthanide alkyl + H_2.[26] It has generally been assumed that such differences are due to the "soft" nature of the P center relative to the "hard" La metal catalytic center.[27]

(25) See: R. F.; Dutoi, A. D.; McConnell, K. W.; Naylor R. M. *J. Am. Chem. Soc.* **2001**, *123*, 2839−2848.

(26) Jeske, G.; Lauke, H.; Mauermann, H.; Swepston, P. N.; Schumann, H.; Marks, T. J. *J. Am. Chem. Soc.* **1985**, *107*, 8091−8103.

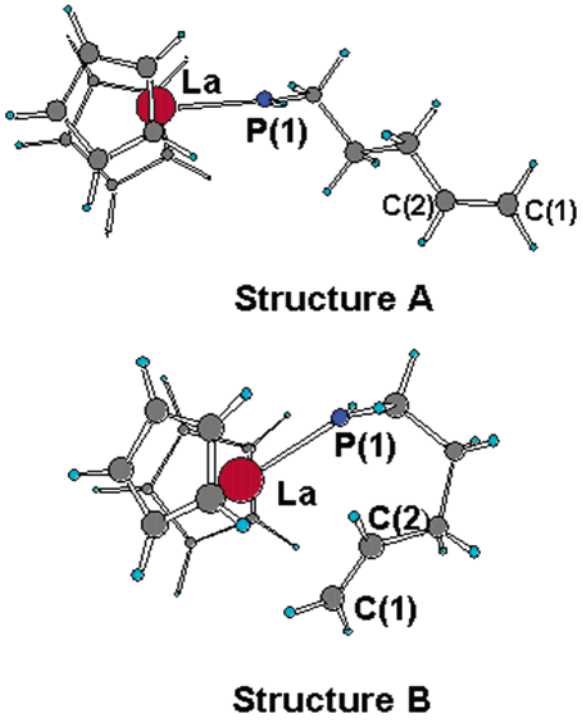

Figure 2. Optimized molecular structures of the activated catalyst $(C_5H_5)_2LaPH(CH_2)_3CH{=}CH_2$.

Catalytic Cycle. The catalytic process will be examined through two component steps: namely (i) cyclization and (ii) protonolysis.

(a) Cyclization Step. Similarly to what was established for the parent hydroamination process, hydrophosphination involves rearrangement of the initially activated catalyst (Figure 2, structure A) to the more stable (3.6 kcal/mol) configuration B (Figure 2).

The latter structure permits closer approach of the olefin π system to the electrophilic La center (hence coordinative saturation) and, as a consequence, prepares the system for cyclization. The stabilization of structure B vs structure A on the hydrophosphination reaction coordinate finds an identical counterpart in the hydroamination reaction coordinate ($\Delta E = 0.1$ kcal/mol for P vs N), since this rearrangement does not involve the heteroatom to any significant degree.

Insertion of the C=C double bond into the La−P linkage occurs in the cyclization transition state, and the four-membered La−P(1)−C(2)−C(1) metallacycle (Figure 3) is found to have a 10.7° folding angle (Table 2). In this geometry, the La−P(1) and the C(1)=C(2) bonds are eclipsed. A similar geometry is found in the olefin insertion step into the La−C bond in analogous polymerization processes.[18h] The data reveal that, as cyclization proceeds, there is concerted lengthening (relative to the activated catalyst) of the La−P(1) and C(1)−C(2) distances as the direct bonding evolves into an La−phosphine dative interaction, while the C=C double bond acquires single-bond character. Simultaneously, there is contraction of the P(1)−C(2) distance as cyclization progresses. The data in Table 2 show that

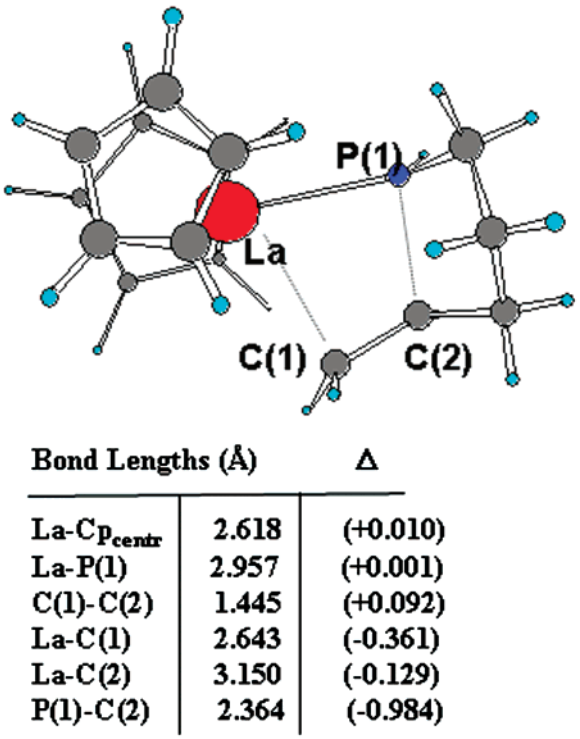

Figure 3. Optimized molecular structure of the hydrophosphination/cyclization transition state.

Table 2. DFT-Derived Bond Lengths (Å) and Bond Angles (deg) of the Molecular Structures Involved in the La−$PH(CH_2)_3CH{=}CH_2$ Cyclization Step[a]

	activated catalyst **B**	cyclization transition state	cyclization product
	Bond Lengths		
La−Cp$_{centr}$	2.608	2.618	2.620
La−P(1)	2.956	2.957	3.168
La−C(1)	3.004	2.643	2.611
La−C(2)	3.279	3.150	3.343
P(1)−C(2)	3.348	2.364	1.911
C(1)−C(2)	1.353	1.445	1.540
	Bond Angles		
Cp−La−Cp	133.3	135.0	133.9
	Torsion Angles		
Cp−La−Cp−P(1)	43.6	31.4	17.3
La−P(1)−C(2)−C(1)	−6.9	−10.7	−21.6

[a] The other geometrical parameters are not significantly affected.

the lengths of the La−P(1), C(1)−C(2), and P(1)−C(2) bonds in the cyclization transition state (Figure 3) are approximately intermediate between those observed in the reagents and products, while the La−C(1) distance lies closer to that in the product. IRC calculations of 12 points around the cyclization transition state provide quantitative details of such variations, and the data in Table S14 show that the La−P(1) and C(1)−C(2) distances increase 0.004 and 0.049 Å, respectively, while the P(1)−C(2) distance decreases 0.217 Å, indicating that the principal geometrical evolution in this step is the actual ring closure. There is also a profound coordinative reorganization about the La^{3+} ion as the hydrophosphination/cyclization reaction coordinate is

(27) (a) Pearson, R. G. *J. Chem. Educ.* **1987**, *64*, 561−567. (b) Ho, T.-L. *Hard and Soft Acids and Base Principles in Organic Chemistry*; Academic Press: New York, 1997. (c) Pearson, R. G. *Hard and Soft Acids and Bases*; Dowden, Hutchinson, and Ross, Inc.: Straudsburg, 1973.

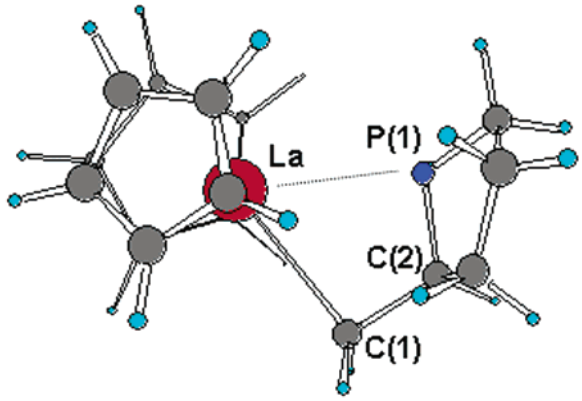

Structure C

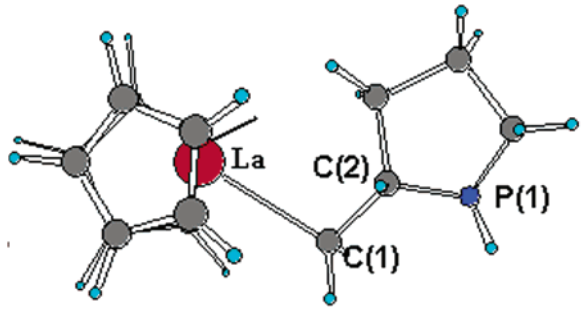

Structure D

Figure 4. Optimized molecular structures of the hydrophosphination/cyclization products. In structure **C**, the hydrogen atom on P(1) is obscured from view by the phosphorus atom.

traversed. First, there is a progressive and pronounced elongation of the La−P(1) bond, reflecting evolution from a strong phosphido La−P(H)R σ-bond to a formal La←P(H)RR′ dative interaction. A similar progressive shortening of the P(1)−C(2) distance is observed due to the olefin insertion process and subsequent formation of the σ-bonded phosphinacyclopentyl product.

The cyclization product is found to assume either of two conformations, differentiated by the coordinative details of the P-phosphine interaction with the lanthanide ion (Figure 4). Optimized structures **C** and **D** are depicted in Figure 4. The P-coordinated structure **C** is found to be 13.1 kcal/mol more stable than structure **D** and represents the initial direct insertion product. Note that two homologous structures are also found along the hydroamination reaction coordinate[28] with a somewhat greater enthalpic difference for hydroamination (16.4 kcal/mol). The difference in stabilization found between the hydrophosphination and hydroamination products (ΔE = 3.3 kcal/mol) is an indication of a stronger "hard−hard" La−N(amine) interaction versus a "hard−soft" La−P (phosphine) coordination. The complete hydrophosphination/cyclization energetic profile is displayed in Figure 5, with relevant energetic data summarized in Table 3. Interestingly, the insertive step ii of the hydrophosphination/cyclization process proceeds with a lower barrier than in the corresponding hydroamination/cyclization process (vide infra) with a more stable transition state (by 4.6 kcal/mol) and an initial cyclization product which is 3.4 kcal/mol more stable (Table 3). The present differences in the energetic profile vis-á-vis hydroamination can be explained by the aforementioned energetic differences accompanying ring formation. In the phosphorus case, the smaller heterocyclic ring strain is evident, since the larger covalent radius and different bonding tendencies of the P center relax the structure (vide supra).

Computed energetic pathways as a function of solvent along the cyclization reaction coordinate are summarized in Table 4. The relative energies are referred to structure **B** of the activated catalyst. The data show that, in noncoordinating benzene, toluene, and heptane, hydrophosphination/cyclization energetics are relatively insensitive to solvation, with the barriers to cyclization and protonolysis slightly greater and with the final product slightly more stable. This result is consistent with experimental data showing minimal solvent effects on rate and stereochemistry, except in coordinating solvents.

(b) Protonolysis Step. The La−C protonolysis process (Scheme 1, step iii), following cyclization, regenerates the catalyst and releases the cyclophosphine product. Thus, (i) a second substrate molecule (here simulated by methylphosphine) coordinates to the lanthanum center (Figures 6a,b), (ii) proton transfer occurs from the bound $-PH_2$ group to the Ln−hydrocarbyl, thus creating a Ln−phosphido complex stabilized by coordinative interaction with an additional P lone pair (Figure 6c), and, finally, (iii) the phosphinacycle undergoes dissociation, regenerating the active catalyst (Figure 6d).

Coordination of the new, second substrate molecule (CH_3PH_2) is accompanied by a sizable energetic stabilization (−6.9 kcal/mol) of the system with respect to the initial cyclization product (Table 3). This highlights crucial and distinctive differences between hydroamination and hydrophosphination (Figure 7). In the analogous hydroamination step, −18.6 kcal/mol stabilization is computed, −11.7 kcal/mol *more exothermic* than for hydrophosphination (Table 3). This, in turn, displaces the overall energetic profile of the protonolysis step in hydrophosphination to higher energies, with the obvious consequence being a slower (than hydroamination) protonolytic activation of the phosphinoalkyl. Enthalpically, this process then becomes the turnover-limiting step for hydrophosphination. While hydroamination involves similar stabilization associated with both coordination of the second amine substrate and with amine coordination in the cyclized product (ΔE = 2.2 kcal/mol), the stabilization in hydrophosphination due to the second substrate is markedly less than that due to the phosphine coordination in the cyclized product (ΔE = 6.2 kcal/mol). In this step, the approach of the second substrate finds the catalytic metal center already engaged in both hydrocarbyl coordination and a dative interaction with the cyclized substrate. The soft−hard character of the interaction between the La^{3+} ion and the P compared with the hard−hard interaction between the La^{3+} ion and the N doubtless play a role in stabilization. The charge distribution in this step (Table 5) reveals a marked difference between the charge localized on the P atom in hydrophosphination vs that localized on the N atom in hydroamination. In particu-

(28) Motta, A.; Lanza, G.; Fragalà, I. L.; Marks, T. J. *Organometallics* **2004**, *23*, 4097−4104.

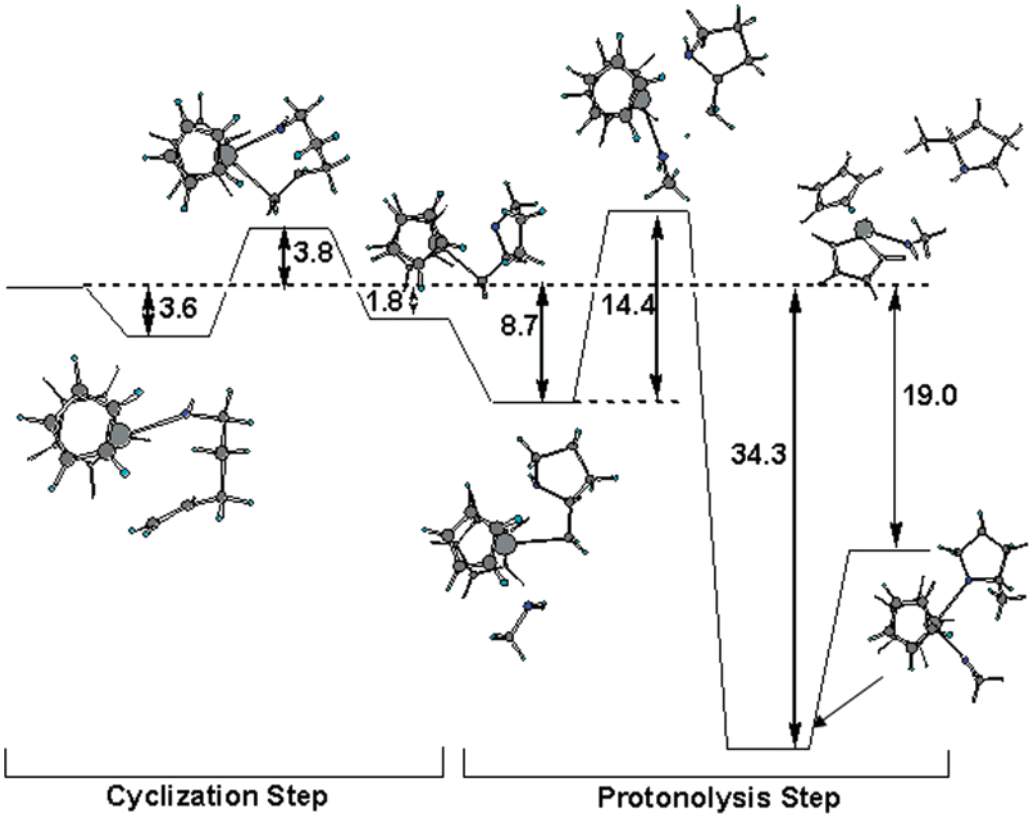

Figure 5. Energetic profile (kcal/mol) for the lanthanocene-mediated hydrophosphination/cyclization pathway. The energies of the isolated reactants are always assumed as references for the energy scale.

Table 3. Relative SCF Energies, Enthalpies, Gibbs Free Energies, and Entropies for the Entire Cyclization/Hydrophosphination Process for $CH_2{=}CH(CH_2)_3PH_2$ Catalyzed by the $(C_5H_5)_2LaCH(TMS)_2$ System

	ΔE (kcal/mol)		ΔH (kcal/mol)	ΔG (kcal/mol)	ΔS (cal/(mol K))
activated catalyst struct **A**	0.0	0.0[a]	0.0	0.0	0.0
activated catalyst struct **B**	−3.6	−3.5[a]	−3.8	−0.9	−9.7
cyclization transition state	3.8	8.4[a]	2.6	8.1	−18.5
cyclization product	−1.8	1.6[a]	−2.5	1.6	−13.5
phosphine complex	−8.7	−17.0[a]	−7.8	7.1	−50.3
protonolysis TS	5.7	−4.2[a]	4.8	21.6	−56.2
phosphine−phosphido complex	−34.3	−32.3[a]	−30.8	−17.0	−46.1
final product	−19.0	−13.8[a]	−16.8	−15.3	−5.0

[a] Referenced to the hydroamination analogue.

Table 4. Relative SCF Energies (kcal/mol) in the Hydrophosphination/Cyclization Reaction Pathway for Different Solvents

	vacuum	toluene (ϵ = 2.379)	benzene (ϵ = 2.247)	heptane (ϵ = 1.92)
activated catalyst **B**	0.0	0.0	0.0	0.0
cyclization TS	7.4	8.8	8.7	8.4
cyclization product	1.8	2.7	2.5	2.7
phosphine complex	−5.1	−2.9	−3.0	−3.3
protonolysis TS	9.3	11.4	11.3	10.9
phosphine−phosphido complex	−30.7	−29.7	−29.7	−29.9
final product	−15.4	−20.3	−20.2	−18.5

lar, there is a greater electrostatic contribution to the La−N interactions than to the La−P interactions (Table 5). There is no evidence of other effects which could account for the smaller stabilization energy associated with the uptake of the second phosphine substrate.

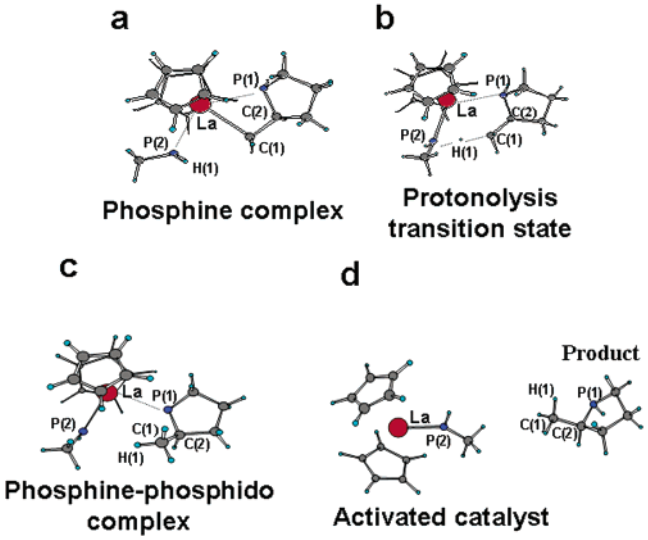

Figure 6. Optimized molecular structures of the phosphine−hydrocarbyl complex, protonolysis transition state, and phosphine−phosphido product.

The proton-transfer process is similar for both hydroamination and hydrophosphination. In the transition state (Figure 6b), H^+ transfer from CH_3PH_2 to the La−C(1) linkage of the cyclic product is synchronized with the approach of CH_3PH_2 to the electrophilic Ln metal center. Along the P(2)- - -H(1)- - -C(1) vector associated with proton transfer (Figure 6b), the P(2)−H(1) distance is 0.260 Å longer than in the methylphosphine complex and the evolving H(1)−C(1) length is 0.563 Å longer than in the phosphine−phosphido protonolysis product.

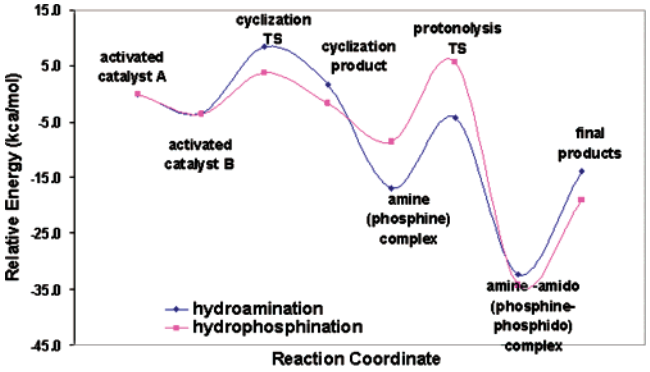

Figure 7. Lanthanocene-mediated hydrophosphination/cyclization SCF energy profile compared with that for analogous hydroamination/cyclization. Labeling is for the hydroamination case.

Table 5. Selected NBO Atomic Charges for the Amine Complex in the Hydroamination and for the Phosphine Complex in the Hydrophosphination[a]

	amine complex	phosphine complex
La	+2.484	+2.409
E(1)	−0.832	+0.431
E(2)	−0.993	+0.224
Cp	−0.854	−0.830

[a] E = N, P. Labeling refers to the structure in Figure 6a for the hydrophosphination case.

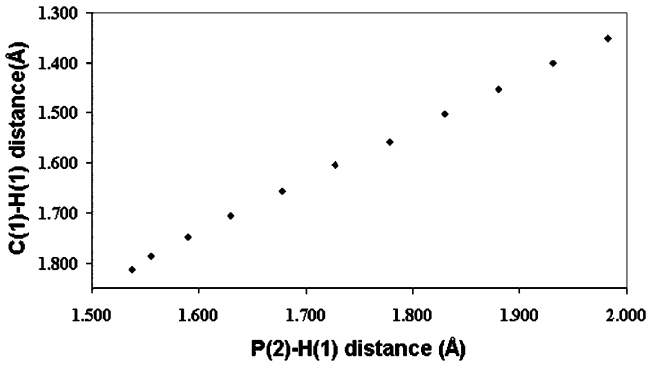

Figure 8. Correlation between the P(2)−H(1) distance and H(1)−C(1) distance in the protonolysis step of hydrophosphination/cyclization.

The results of IRC calculations on 10 points around the protonolysis transition state correlate well with the dynamics of the process and provide quantitative details on such variations. Thus, quantitative data (Table S15) show that elongation of the P(2)−H(1) bond (0.444 Å) is comparable to the decrease in C(1)−H(1) distance (0.462 Å). Moreover, there is a linear correlation (Figure 8) between changes associated with the P(2)−H(1) distance and C(1)−H(1) length, providing convincing evidence for a concerted bond-breaking/bond-forming process.

The protonolysis kinetic product is found to have a pseudotetrahedral architecture around the Ln^{+3} ion (Figure 6c). The Cp_2Ln moiety has a direct phosphido bonding interaction (2.867 Å), derived from the P(2) methylphosphine protonolysis agent, as well as a dative contact (3.199 Å) with P(1) of the cyclic phosphine. The new Ln−P(2) bond is therefore metrically comparable to the Ln−P(1) distance (2.956 Å) in the initial activated catalyst (Figure 2), while the Ln−P(1) distance in the

Table 6. DFT Bond Lengths (Å) and Bond Angles (deg) of Structures Involved in the Hydrophosphination Protonolysis Step

	phosphine-coordinated complex	protonolysis transition state	phosphine−phosphido complex
	Bond Lengths		
La−Cp_{centr}	2.643	2.616	2.611
La−P(1)	3.203	3.188	3.199
La−P(2)	3.199	3.083	2.867
La−C(1)	2.674	2.838	4.599
P(2)−H(1)	1.417	1.677	3.530
C(1)−H(1)	3.564	1.657	1.094
	Bond Angles		
Cp−La−Cp	133.2	132.1	133.9
P(1)−La−P(2)	127.5	122.1	94.3
	Torsion Angles		
Cp−La−Cp−P(1)	60.8	65.7	39.1

phosphine−phosphido kinetic product is close to that (3.203 Å) in the inserted phosphine complex (Figure 6a,c). Note that the direct phosphido bond is, not surprisingly, 0.332 Å shorter than that of the weaker "dative" phosphine contact (Table 6). The energetic profile for the hydrophosphination/cyclization protonolysis step is shown in Figure 5, and data are summarized in Table 3. There is evidence that the phosphine complex (Figure 6a) is markedly less stable then the analogous amine complex (ΔE = 8.3 kcal/mol), considering the rather labile La−P bonding versus the stronger La−N interaction (vide supra). This induces possible competition in the catalyst environment between interactions involving either the second substrate or the cyclized product. In contrast, this competition is negligible in the analogous hydroamination step, with the obvious consequence of kinetic inhibition by the cyclized product, as experimentally observed in the hydrophosphination case.[11c] Further insights into this intriguing aspect of the mechanism are obtained from direct evaluation of the stabilization energies due to the two competing interactions. Thus, hydroamination involves substrate stabilization due to interaction with the second incoming substrate (−18.6 kcal/mol) markedly greater than with the cyclized product (−11.0 kcal/mol). In contrast, both processes are competitive in hydrophosphination with comparable stabilization energies: −8.8 kcal/mol for the cyclized product and −6.9 kcal/mol for the second substrate. The transition state energy for protonolysis relative to the phosphine−alkyl complex (14.4 kcal/mol) is similar to that calculated for the hydroamination case (12.8 kcal/mol; Table 3). These smaller disparities reflect the relatively low stability of the phosphine complex that, in turn, influences the transition state (Figure 7). Nevertheless, the transition state for protonolysis associated with hydroamination lies significantly lower in energy than the cyclization products (−5.8 kcal/mol), while the corresponding protonolytic hydrophosphination transition state lies significantly higher (+7.5 kcal/mol). Therefore, protonolysis effected by the phosphine substrate is more sluggish than the analogous process for the amine, in good agreement with experiment.[11c] Note also that the data in Figure 7 show that the energetic maxima on the respective hydroamination and hydrophosphination reaction coordinates are similar in magnitude and that the scenarios associated with the maximum positioned in either the cyclization or protonolysis manifold are not

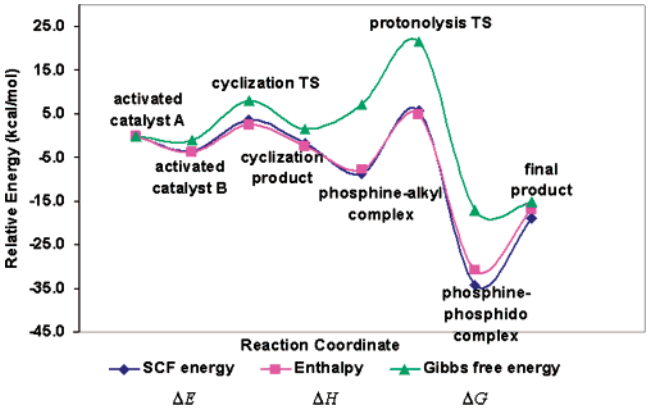

Figure 9. Thermodynamic profiles of the phosphinoalkene hydrophosphination/cyclization pathway. The energies of isolated reagents are always assumed as references for the energy scale.

inconsistent with observed rate laws, which are both initially zero-order in substrate.[7,11]

The kinetic protonolysis product in the hydrophosphination process is stabilized by 34.3 kcal/mol (Table 3) compared to 32.3 kcal/mol in the hydroamination case. The minor steric crowding found in both kinetic protonolysis products (Figure 6c for phosphination) with respect to the phosphine/amine complexes (Figure 6a for phosphination) affords a comparable stabilization in both cases. The final elimination of cyclized product requires 15.3 kcal/mol in hydrophosphination and 18.5 kcal/mol in hydroamination (Table 3), in close agreement with both theoretical and experimental findings[11c,28] that indicate weaker coordination of the substrate P center relative to the corresponding N heterocycle. Calculated energies, corrected for solvent effects, for the protonolysis step are reported in Table 4. Similar to the cyclization step, solvation does not substantially affect the reaction profile. The data in Table 4 evidence only moderate stabilization with respect to vacuum (3.1−4.9 kcal/mol) of the final product in the solvents examined. The other energetic parameters are only marginally affected (∼2 kcal/mol) by solvation effects.

Thermodynamics of the Hydrophosphination/Cyclization Reaction. Thermodynamic state functions (enthalpy, Gibbs free energy, and entropy) associated with the stationary states as well as with the transition states of the hydrophosphination/cyclization process are compiled in Table 3 and displayed in Figure 9. It can be seen that the enthalpic profile (ΔH_{298}) is entirely superposable on that of the SCF results discussed in the previous section. In contrast, the Gibbs free energy (ΔG_{298}) profile differs markedly due to entropic contributions ($-T\Delta S_{298}$). In fact, there is a monotonic decline in entropy (Table 3) due to the progressive loss of degrees of freedom along the reaction coordinate.

Greater in magnitude is the decrease in entropy associated with formation of the phosphine complex (Figure 6a; $\Delta S = -50.3$ cal/(mol K))—the entropic change is due to the bimolecular association to form a single complex (two particles → one). The modest $\Delta H^{\ddagger}_{298}$ value (−7.3 kcal/mol) in the protonolysis step suggests a concerted transition state, with significant bond formation to compensate for simultaneous bond scission (vide supra). The large, negative $\Delta S^{\ddagger}$ value (−42.7 cal/(mol K)) is consistent with a highly organized, polar transition state in which a significant loss of internal degrees of freedom occurs, in excellent agreement with experiment[11c] (Table 3). Finally, the release of products and regeneration of the catalyst involves a sizable entropic gain. This entropic contribution significantly affects the overall ΔG trend, with the consequence that related values shift to higher energies (hence to less favored processes) relative to the corresponding potential energies. These results implicate a phosphine−phosphido complex as the likely resting state of the catalyst, in good agreement with experiment.[11c]

Concluding Remarks

The catalyst generation and hydrophosphination/cyclization processes promoted by the highly electrophilic $(C_5H_5)_2La-$ catalyst have been investigated using DFT and analytical gradient methods to understand catalytic reaction pathways and related reaction energetics. It is found that the insertive cyclization step is essentially thermoneutral ($\Delta H = -2.5$ kcal/mol), while the subsequent concerted protonolysis step (concerted bond-breaking/bond-forming process) is exothermic ($\Delta H = -16.8$ kcal/mol), in complete accord with experimental data. In terms of the kinetics of the various components of the catalytic cycle via-à-vis hydroamination/cyclization, the computations show that C=C insertion into the La−heteroatom bond is turnover-limiting for hydroamination while La−C protonolysis is turnover-limiting for hydrophosphination. Moreover, the energetic maxima of the two reaction coordinates are nearly coincident, in good agreement with experiment. Nevertheless, note that the experimental data suggest that the lower hydrophosphination protonolytic reactivity does not greatly affect the observed catalytic cycle and the derived rate law to any great extent. Noncoordinating solvents such as benzene, toluene, and heptane do not significantly affect the reaction pathway. Future studies will focus on the nature of organolanthanide-mediated hydroelementation pathways as a function of C−C unsaturation and of the lanthanide catalytic center.

Acknowledgment. This research was supported by the Ministero dell'Università e della Ricerca Scientifica e Tecnologica (MURST Rome), the Consiglio Nazionale delle Ricerche (Rome), and by the U.S. National Science Foundation (Grant No. CHE-0415407).

Supporting Information Available: A complete list of Cartesian coordinates of all structures and data from IRC calculations presently analyzed. This material is available free of charge via the Internet at http://pubs.acs.org.

OM050570D